Development of intimate contact during processing of carbon fiber reinforced Polyamide-6 tapes

P. M. Schaefer, T. Guglhoer, Markus G. R. Sause, K. Drechsler

Angaben zur Veröffentlichung / Publication details:

Schaefer, P. M., T. Guglhoer, Markus G. R. Sause, and K. Drechsler. 2017. "Development of intimate contact during processing of carbon fiber reinforced Polyamide-6 tapes." *Journal of Reinforced Plastics and Composites* 36 (8): 593–607. https://doi.org/10.1177/0731684416687041.

Development of intimate contact during processing of carbon fiber reinforced Polyamide-6 tapes

PM Schaefer[1], T Guglhoer[2], MGR Sause[2] and K Drechsler[1]

Abstract

Contact development between the surfaces of two tapes is considered as a critical step in processing carbon fiber reinforced thermoplastic composites. In this study, the development of intimate contact between carbon fiber reinforced Polyamide-6 (PA-6) tapes is investigated experimentally using consolidation experiments and X-ray computed tomography for quantitative contact characterization. The experimental results indicate that the development of intimate contact occurs in the range of seconds even when temperatures are only slightly above the melting temperature and applied pressures is in the range of 1-4 kPa. Experimental data are compared with the results of the two analytical models proposed by Lee and Springer as well as Yang and Pitchumani. Both models overestimate the time needed to reach full contact for the PA-6 tape. In comparison to previously investigated PEEK materials, PA-6 has a relatively low viscosity and the tapes possess a resin-rich layer near the surface, which seems to influence the contact development process. Besides the assumptions made for viscosity, the sensitivity to input parameters describing the surface topology strongly influence the model results and the accuracy of predictions.

Introduction

Carbon fiber reinforced thermoplastics have seen an increasing acceptance in recent years. Especially, fully impregnated semi-finished products such as tapes and organic sheets have led to possibilities for new manufacturing processes such as thermoplastic automated tape placement (ATP). ATP is a process which is used either to manufacture entire parts with tailored mechanical properties or to reinforce parts locally. For example, ATP has been successfully used to manufacture large-scale vessel structures[1] or to add local reinforcements to press-formed thermoplastic parts.[2] For both processes—constructing or reinforcing construction elements—unidirectional (UD) reinforced tapes are placed layer by layer to build up a laminat, in which each layer is bonded to the previous one. This process of adding one layer to another consists of three consecutive phases: First, the layers are heated up to melting temperature using different heat sources such as hot gas, open flames, or laser irradiation; second, the layers are consolidated by applying pressure to the material; third, the laminate is cooled down until the matrix solidifies.[3] During the consolidation phase two phenomena occur: contact development between two rough tape surfaces (i.e. intimate contact) and, subsequently, the process of autohesion, also known as healing or polymer chain diffusion, begins.[3–6]

The first ATP machines were efficient in placing tape material; however, they did not ensure complete consolidation. Therefore, a post-consolidation step in an autoclave was necessary. More recently, improvements

[1]Chair of Carbon Composites, Department of Mechanical Engineering, Technical University of Munich, Garching, Germany
[2]Experimental Physics II, Institute of Physics, University of Augsburg, Augsburg, Germany

Corresponding author:
T Guglhoer, Experimental Physics II, Institute of Physics, University of Augsburg, Universitätsstrasse 1, D-86135 Augsburg, Germany.
Email: thomas.guglhoer@physik.uni-augsburg.de

in the ATP machines—especially the development of precise laser heat sources—allow the online consolidation of thermoplastic materials without a cost-intensive post-consolidation in an autoclave, as studies on laboratory scale have shown.[1,2] In addition, the development of a variety of new tape materials, using low-cost engineering plastics (e.g. Polyamides) instead of expensive high-performance materials (e.g. Polyetheretherketone, PEEK) could expand the fields of application and increase the economic attractiveness of ATP processes for other industries than aerospace.

For further improvements in thermoplastic ATP processes, the material behavior during consolidation and its physical processes ought to be fundamentally understood. In this paper, we will contribute to this goal by exploring the development of intimate contact. The intimate contact is an important factor, as previous research[3,7,8] suggests and it substantially affects the processing times. Being able to model the development of intimate contact allows predicting the optimal processing parameters. These models can also be used to estimate the bonding strength of welded thermoplastic materials[7,9,10] and are applied in the numerical process optimization.[11]

Therefore, in this paper we address the following questions: how fast does full intimate contact develop for carbon fiber reinforced Polyamide-6 (PA-6) tapes? Are current models capable of predicting the contact development between industrial grade carbon fiber reinforced PA-6 tapes? Which problems may arise due to the acquisition of the model parameters? Since PA-6 has a lower viscosity than thermoplastics used in earlier studies on intimate contact, we also address the following question: Are there specific limitations of current models for the industrial grade carbon fiber reinforced tape with a low-viscous PA-6 matrix?

In order to answer these questions, we will first outline different models that are currently used to explain the development intimate contact. As the literature reveals large differences in the model parameters,[7,12,13] we will also focus on the methods used to acquire the input parameters for the Lee and Springer[13] model as well as for the Yang and Pitchumani[14] model. Second, in the experimental part, we will present material properties and model parameters for a carbon fiber reinforced PA-6 tape material. In particular we will address the influence of viscosity, as this property of the investigated material significantly differs from that of PEEK, which was explored in the previous studies.[7,12–14] Furthermore, we will present the experimental results in which the development of intimate contact over time was determined. The investigated samples were manufactured in consolidation experiments and later evaluated using X-ray computed tomography. Third, we will describe the results derived from two analytical models and compare the models' results with our experimental data. Finally, we will address the limitations of the current models such as their sensitivity to the surface parameters and we will discuss limitations, which arise for the investigated low-viscous matrix material.

Analytical intimate contact models

Over the last 30 years, different models for the development of intimate contact have been proposed. The most commonly used models are the statistical rectangle model by Dara and Loos,[15] the identical rectangle model by Lee and Springer,[13] and the fractal model by Yang and Pitchumani.[14] All models have in common that the contact between two adjacent layers—the degree of intimate contact D_{IC}—of thermoplastic materials is quantified by the ratio of physical contact area and the projected surface area, which yields unity when full contact is established

$$D_{IC} = \frac{surface\ in\ contact}{projected\ surface\ of\ material} \tag{1}$$

Furthermore, all models incorporate two main ideas: First, the description of the rough tape-surface and second, the leveling of the surface asperities due to matrix flow, when pressure is applied to the tapes. Nevertheless, the intimate contact models differ in the used surface sub-models. Figure 1 shows a schematic representation of the described surface models. In the following section, we review these models in more detail.

Statistical rectangle model by Dara and Loos

The first description for the development of contact between thermoplastic sheets was published by Dara and Loos in 1985.[15] They described the surface of rough thermoplastic prepregs as a statistical distribution of rectangles with different heights and widths. As fibers are orientated unidirectionally in the tapes, the surface roughness is reduced to a two-dimensional model in the plane perpendicular to the fiber direction.

The different sizes of rectangles were obtained from micrographs and the authors found that the height of theses rectangles can be represented by a Weibull distribution. The degree of contact was calculated from the cumulative distribution assuming a viscous squeeze flow of the molten composite.

This model offered a precise representation of the tape surface; however, the effort for obtaining the surface-model parameters was enormous and implementing a flow model was difficult. Therefore, the model was simplified by Lee and Springer.

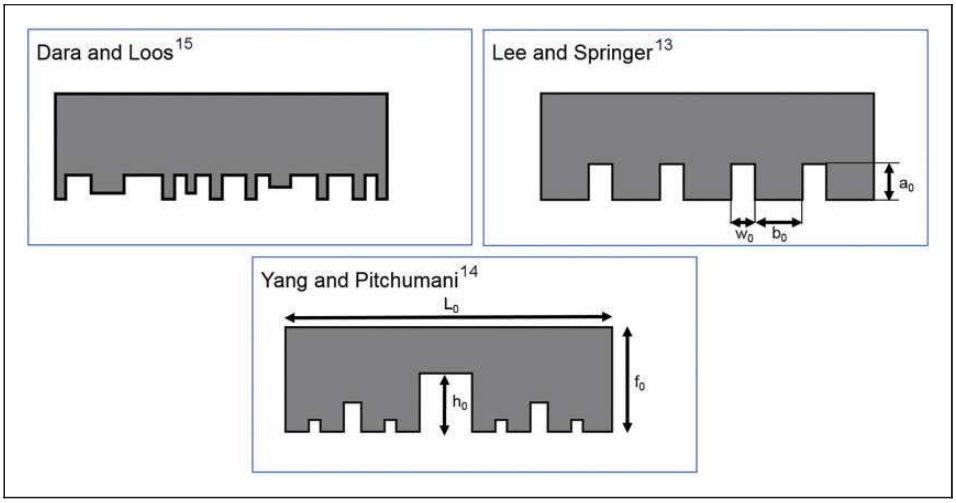

Figure 1. Schematic representation of surface models.

Identical rectangle model by Lee and Springer

Lee and Springer[13] also represent the surface of a rough tape as series of rectangles; however, they assumed all rectangles to be of identical height a_0 and width b_0. These rectangular asperities are separated by gaps of width w_0. Lee and Springer were the first authors to introduce the term "degree of intimate contact" D_{IC}. The assumption of identical rectangle dimensions also simplifies the flow model, which describes the deformation of the asperities and the filling of the gaps in between. Lee and Springer propose a Newtonian one-dimensional flow of the asperities into the gaps. The evolution of intimate contact as a function of the applied pressure P_{app}, and the temperature-dependent viscosity η is given by

$$\mathrm{D}_{IC} = \frac{1}{1+\frac{w_0}{b_0}}\left[1+5\left(1+\frac{w_0}{b_0}\right)\left(\frac{a_0}{b_0}\right)^2\int_0^{t_c}\frac{P_{app}}{\eta(T)}\mathrm{d}t\right]^{\frac{1}{5}} \quad (2)$$

where the geometrical parameters w_0, b_0, and a_0 are shown in Figure 1. The initial contact is established at $t = 0$ and contact development continues until $t = t_c$. Lee and Springer also published an initial set of material parameters for the viscosity and the surface parameters of PEEK APC 2. The geometrical parameters were obtained from micrographs of unconsolidated plies and values for the mixed fiber–matrix viscosity were used as provided by the material manufacturer.

The contact model was first applied by Mantell and Springer[12] for the process simulation of the thermoplastic winding processes. Levy et al.[16] also used the Lee and Springer model for their study. They obtained the surface parameters by fitting the model parameters to experimentally obtained values for D_{IC}. Lee and Springer also experimentally validated their model and obtained large contact times of 50 to 200 s for the PEEK AS4 tape material APC-2 at typical processing temperatures and for a pressure of a few hundred kPa.

Fractal model by Yang and Pitchumani

As the representation of a rough surface as identical rectangles is a very simplified approach, Yang and Pitchumani[14] proposed a more sophisticated representation of the tape surface. They described the morphology of the tape as a Cantor set fractal surface showing multiple generations of asperities with decreasing height. They implemented a squeeze flow model, in which the smallest asperities of the highest generation are squeezed without any deformation of the larger rectangles. Once the gaps of the highest generation are filled, the previous generation of asperities begins to deform. The full contact is reached as soon as the gaps of the first generation are filled.

The evolution of intimate contact for the n^{th} generation of asperities is described by

$$\mathrm{D}_{IC}^{(n)} = \frac{1}{f^n}\left[\frac{5}{4}\left(\frac{h_0}{L_0}\right)^2\frac{f^{\frac{2n\mathrm{D}}{2-\mathrm{D}}+n+4}}{(f+1)^2}\int_{t_{n+1}}^{t_C}\frac{P_{app}}{\eta(T)}\mathrm{d}t+1\right]^{\frac{1}{5}} \quad (3)$$

Comparing equations (2) and (3), one can conclude that the deformation of each generation of asperities as a function of pressure and viscosity is described in similar ways in both models: the fractal model by Yang and Pitchumani and the Lee and Springer model. The main advantage of the Yang and Pitchumani approach is that the surface parameters f, h_0, L_0, and D can be obtained directly from surface profile measurements.

However, it is presumed that the surface exhibits fractal characteristics, which is not necessarily true for all tape materials. The model can therefore not be applied universally to all tape materials.

Material characterization

In the following we describe a study, in which we focused on the intimate contact models by Lee and Springer as well as Yang and Pitchumani. The two models are the most relevant for process modeling, because in the previous studies[13,14] they have yielded good results and the surface parameters can be determined directly from measured surface profiles. We started by determining the characteristic material parameters for both models.

Lee and Springer as well as Yang and Pitchumani consider the influence of surface roughness on the development of intimate contact. Appropriate input parameters can be obtained from surface profiles. In our study, we measured surface profiles via tactile profilometry. For the surface characterization a Dektak 6 M Stylus profilometer was used. The lateral sampling rate is $1.07\,\mu m^{-1}$ and we chose a measuring length of 50 mm. A typical surface profile is shown in Figure 2. To resolve the resolution limitations of the Dektak 6 M Stylus instrument additional atomic force microscopy (AFM) measurements were performed using a Veeco Dimensions 3100 AFM. AFM profiles were recorded using a scanning length of 80 μm and a sampling rate of $6.4\,\mu m^{-1}$.

Surface parameters Yang and Pitchumani model

The surface parameters for the Yang and Pitchumani model are the fractal dimension of the surface D, the scaling ratio f, the height of the first generation asperity h_0 and the total horizontal length of the Cantor set block L_0. In our study, these parameters were determined according to the suggestions of the original authors.[14] D and L_0 were calculated from the power spectrum obtained by the squared discrete Fourier transformation amplitude from the surface profiles following the recommendations of Elson.[17] For the estimation of the power spectrum, Welch's method[18] was used by applying a Hann window function and using 10 subsamples with an overlap of 50%. The power spectrum of fractal surfaces in a frequency range follows a power law[14]

$$S(\omega) = \frac{C}{\omega^{5-2D}} \tag{4}$$

The fractal dimension D is obtained by the slope m of the power spectrum in a log–log plot, which is related via

$$D = \frac{m+5}{2} \tag{5}$$

For the determination of m results were considered from both types of profilometry measurements: in the low frequency range with respect to Dektak measurements, in the high frequency range incorporating the results of the AFM measurements. L_0 is determined by the inverse of the frequency corresponding to the lower boundary of the linear range ω_0, as shown in Figure 3; the scaling parameter f is obtained using the slope of the total intercepted length of the surface profile and a horizontal line as function of the distance from the mean plane in a range from $-\sigma$ to σ, which is equal to equation (4) in Yang and Pitchumani.[14]

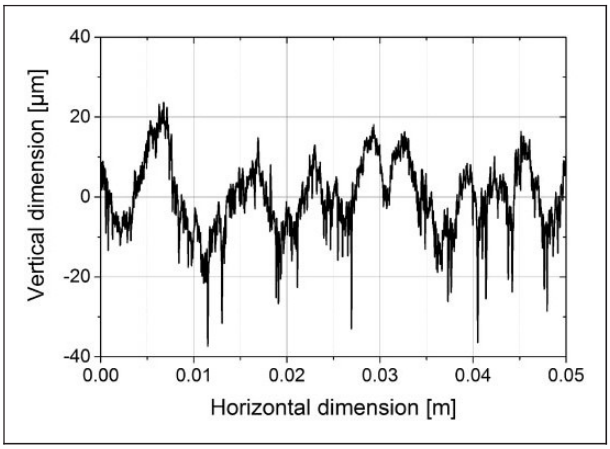

Figure 2. Surface profile of the tape obtained by tactile profilometry.

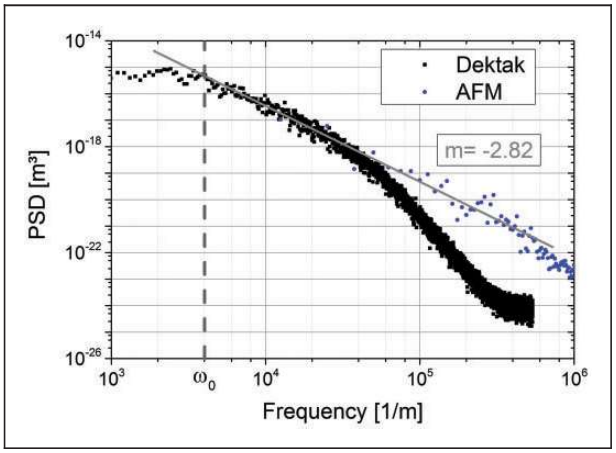

Figure 3. Power spectrum density (PSD) of the surface profiles of Dektak and AFM measurements.

For the evaluation of surface profiles, a length of L_0 was chosen. The height of the first generation asperities h_0 is estimated from twice the root-mean-squared roughness of the surface profile. Since the roughness depends on the evaluation size of the surface profile, the root-mean-squared roughness was evaluated using Parseval's theorem with a minimum frequency of $1/L_0$

$$h_0 = 2 \cdot \left(\int_{L_0}^{\infty} S(\omega) \mathrm{d}\omega \right)^{-1} \tag{6}$$

Surface parameters Lee and Springer model

The surface parameters for the Lee and Springer model constitute: the initial asperity height a_0, the initial asperity width b_0, and the initial width of the gaps between two adjacent asperities w_0. It is needed to calculate the ratios a_0/b_0 and w_0/b_0, which are the input parameters for the development of intimate contact according to equation (2). While Yang and Pitchumani proposed exact proceedings to obtain the geometrical model parameters from the surface characterization of the unconsolidated tapes, a variety of approaches exist for the Lee and Springer model. Lee and Springer proposed to measure the parameters from photomicrographs. In Levy et al.,[16] the model parameters were fitted to minimize the norm 2 error between the model and their experimental results. Grouve et al.[2] used confocal microscopy to obtain the surface roughness profiles and then fitted the results to determine a series of similar rectangles.

In order to utilize the model for the prediction of process parameters or for the evaluation of tape qualities, we propose the following steps to determine the geometric model parameters a priori from surface profiles, which were obtained by tactile measurements (see the previous subsection). The parameter a_0 describes the height of the rectangles and is approximated $\pm 2\sigma$ from the mean surface height where σ is the standard deviation of surface profile. This covers approximately 95% of all surface points (assuming a normal distribution).

For the estimation of the ratio w_0/b_0, an analogy between the identical rectangle model and a rough tape surface is drawn. The surface of the identical rectangle model is represented by n periods each with a period length p (Figure 4). Each of these periodic sections consists of a valley with width w_0 and an asperity with width b_0. The total length of the modeled surface L is equivalent to the measured section of the surface profile. For the analysis of the measured surface profile, a region of interest with a height $\pm 2\sigma$ and length L is defined (Figure 5). Within this region of interest the total area of the material and the area in between,

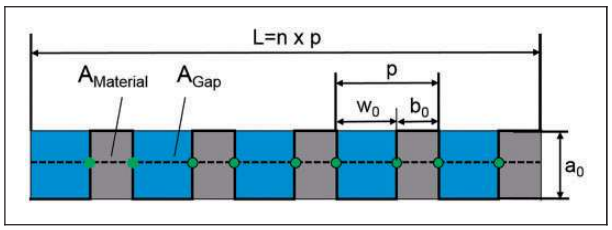

Figure 4. Surface of identical rectangle model.

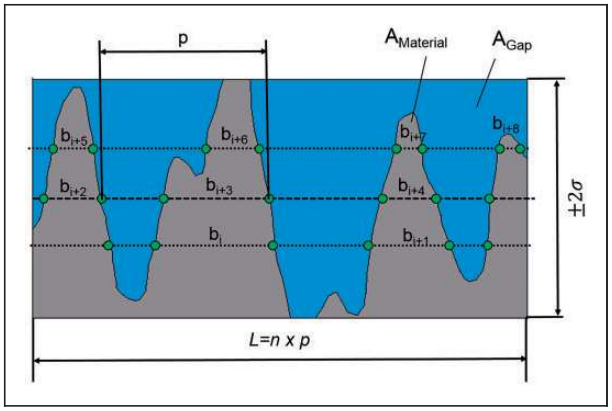

Figure 5. Surface of identical rectangle model.

which is equivalent to the gaps between the material elevations, is determined. From the ratio of these two areas the ratio between w_0 and b_0 can be calculated using equation (7).

In order to determine the average distance between the two gaps of the profile, which is equivalent to b_0, the distance between two intersects (green dots in Figure 5) of the surface profile with a horizontal line (b_i) is calculated at multiple positions. As the value of b_0 highly depends on the vertical position of this reference line, the reference line is moved in steps of 5 µm from bottom to top of the defined region of interest. The mean asperity width b_0 is calculated from the mean of all b_i.

The surface evaluation is performed automatically in a Matlab™ routine

$$\frac{Area_{Gap}}{Area_{Material}} = \frac{na_0w_0}{na_0b_0} = \frac{w_0}{b_0} \tag{7}$$

The results from the surface characterization are summarized in Table 4.

Viscosity measurement

As the viscosity of most of the thermoplastic polymers highly depends on the temperature of the melt, the viscosity is a key input parameter for the intimate contact

models. However, in literature different assumptions are made for the viscosity. Lee and Springer,[13] Mantell and Springer,[12] as well as Yang and Pitchumani[14] suggest using the fiber–matrix viscosity to model the squeeze-flow of the asperities. This suggestion was adopted by Khan et al.[7] for PEEK AS 4 tapes. However, Grouve et al.[2] used the viscosity of neat PPS resin to predict the intimate contact development. It must be noted that the viscosity of the neat resin and that of a fiber-resin mix can vary by orders of magnitude.

Figure 6 shows a micrograph of the carbon fiber reinforced carbon fiber reinforced PA-6 tape used for this study. The image illustrates the existence of resin-rich areas near the surface of the tape. Therefore, for this study we assume that the leveling of asperities by a Newtonian flow is governed by the neat resin viscosity, even though single fibers are sparsely located in this region.

The PA-6 grade, which is used for tape manufacturing, is not available from the supplier. However, we were able to use the neat PA-6 B3K, provided by BASF, which is similar to the polymer, used as matrix in the tapes. The viscosity was measured using a rotational viscometer with plate–plate geometry. The diameter of the plates was 25 mm.

From these measurements, the zero-shear-rate viscosity $\eta_0(T)$ was determined. As the obtained viscosity is used to model the flow of the surface asperities, no additional shear deformation is expected; therefore, the use of the zero-shear viscosity is adequate. An Arrhenius equation was then used to represent the temperature dependency of the viscosity

$$\eta_0(T) = A \exp\left(\frac{E}{RT}\right) \tag{8}$$

In this equation, E is the activation energy, R the universal gas constant, and a fitting parameter A.

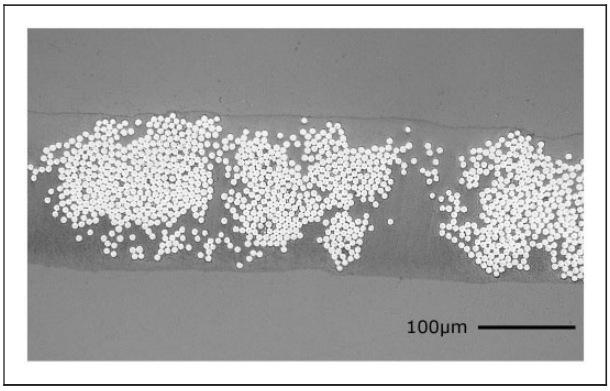

Figure 6. Cross section of the investigated tape.

Consolidation experiments

Consolidation experiments were conducted to obtain the experimental data for the development of intimate contact during processing of carbon fiber reinforced PA-6 tapes. The experimental data show the duration of the contact development for the process optimization and is the basis for the validation of the results obtained by the intimate contact models.

The experiments were conducted with the unidirectional carbon fiber reinforced PA-6 tape material from BASF (B3WC12). The properties of the tape are summarized in Table 1.

Experimental setup

For the validation of the investigated intimate contact models, the three process parameters temperature, pressure, and time had to be controlled during the consolidation experiments. As the viscosity of PA-6 at melt temperature is low compared to other thermoplastic polymers, we expected fast development of full contact. Therefore, short consolidation times as well as fast heating and cooling rates had to be implemented in order to demonstrate the effect of contact development.

Figure 7 illustrates the experimental setup. Similar to the experiments by Levy,[16] weights were used to adjust the consolidation pressure for the experiments. The applied pressure P_{app} was proportional to the height of weights, because the sample area and the material is the same for all weights

$$P_{app} = \rho\, h\, g \tag{9}$$

where g is 9.81 m/s^2. All weights were manufactured from steel. The density ρ of steel is 7.8 g/cm^3. The blocks had a surface area of 60 mm × 60 mm and were machined to reach the exact weight corresponding to 1000 Pa, 2000 Pa, and 4000 Pa, respectively. The weights, which were used for the experiments, are summarized in Table 2.

The experiment consisted of four steps: (1) preheating of metal blocks, (2) preparation of samples, (3) consolidation, and (4) cooling.

Table 1. Material characteristics.

Property	Unit	Value	Error
Fiber volume content	%	47.4	1.2
Tape thickness	mm	0.17	0.01
Density	g/cm^3	1.45	0.02
Melt temperature	°C	221	1,2

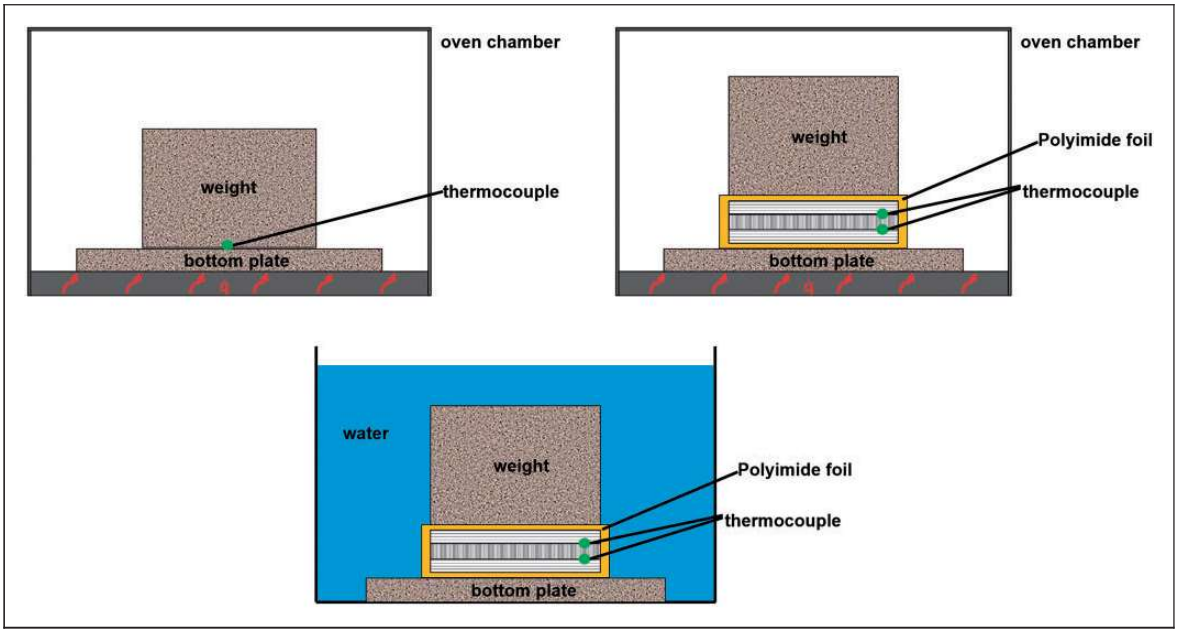

Figure 7. Experimental setup for the consolidation experiments.

Table 2. Properties of the weights used for consolidation experiments.

Weight (g)	Height of weight, h (mm)	Pressure, P_{app} (Pa)
367.0	13.1	1000
733.9	26.1	2000
1467.9	52.3	4000

Preheating of metal blocks. For the consolidation experiments, we aimed for isothermal conditions at 220°C, 225°C, and 230°C, which is at or slightly above the melting temperature of PA-6.[19,20] In order to achieve these conditions the weight and the bottom plate were heated to a specific temperature, which is referred to as pre-heating temperature. For the pre-heating, the plate and a weight were placed in a thermally insulated oven chamber (Figure 7). The oven was heated from its bottom casing. During heating, a thermocouple was placed between the weight and the steel plate to monitor the temperature increase. Once the desired pre-heating temperature was stable, the sample was placed underneath the weight. Due to the high heat capacity of steel pre-heating temperature remained within a range of ±1.5°C while the sample was inserted.

Preparation of samples. Prior to the experiment, the material was dried for 24 h at a temperature of 80°C in a vacuum oven to reduce the effect of de-consolidation.[21] Then the samples were prepared by stacking three layers of tape in 0°/90°/0° orientation. Each layer had a surface area of 60 mm × 60 mm. In order to determine the precise consolidation temperature, a micro-thermocouple with a wire diameter of 80 µm was placed between each contact surface of the stack. These micro-thermocouples were placed near the edge of each sample to prevent any corruption of the contact development by the thermocouple. The entire stack of tape was sealed by a temperature-resistant polyimide foil with a thickness of 25 µm. The thin foil was not likely to thermally insulate the samples.

Consolidation. The consolidation process was started by placing the prepared sample between the weight and the bottom plate. The consolidation time was varied between periods lasting from less than 1 s to periods lasting up to 60 s. For the short periods (i.e. less than 1 s) the setup was removed from the oven immediately after placing the weight on the sample. For the longer period experiments (i.e., up to 30 s) the oven was closed again to prevent larger heat-losses before the entire setup was removed for the cooling phase.

Cooling. According to the different contact models, the evolution of intimate contact can be stopped either by lowering the temperature below a threshold temperature, which is assumed to be the melting temperature T_m for semi-crystalline thermoplastics or by removing the applied pressure. Removing the pressure while the matrix is still in the melting-phase may lead to deconsolidation due to the elasticity of the compressed fiber-bed. Deconsolidation is accompanied by an undesired reduction of intimate contact. Therefore,

the development of intimate contact is terminated by placing the entire setup into a water bath. The use of a water bath for fast cooling requires a good sealing of the samples with polyimide foil. If water flows between the layers it may suddenly evaporate and also lead to deconsolidation.

Figure 8 shows the heating, the isothermal consolidation phase, and the cooling for an experiment with the target temperature of 220°C. The lower boundary refers to the thermocouple between the lower and the middle layer of the sample, whereas the upper boundary refers to the temperature between the upper layer and the middle layer. The weight is placed on the sample after 5 s. A temperature of 210°C is reached approximately after 11 s and the desired target temperature is reached after 20 s, once the weight is placed on the sample. The temperature is kept constant for 17 s after having reached the target temperature. Once the setup is placed into the water, the temperature drops almost instantaneously below the melting temperature. The temperature, which was reached in the isothermal phase, is referred to as the consolidation temperature. The isothermal time period at this temperature is referred to as the consolidation time.

The consolidation time and the consolidation temperature were determined for each sample and for each contact surface individually from the observed temperature profiles. For the consolidation temperature a deviation of ±1.5°C from the target temperature was tolerated, which is approximately the accuracy of the thermocouples. In general, the consolidation time begins when the target temperature is reached and ends when the temperature drops below the target temperature again.

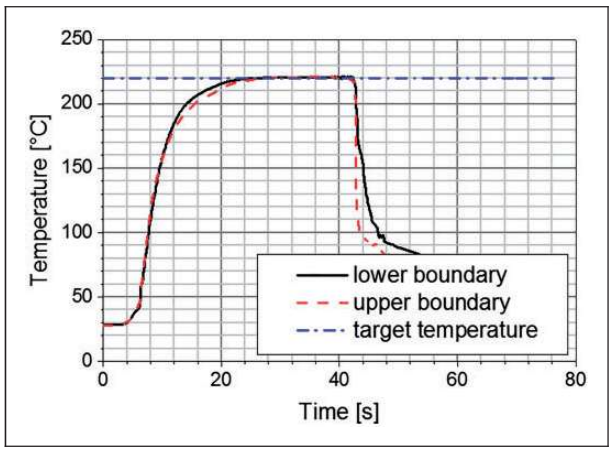

Figure 8. Example for temperature profile during consolidation experiments.

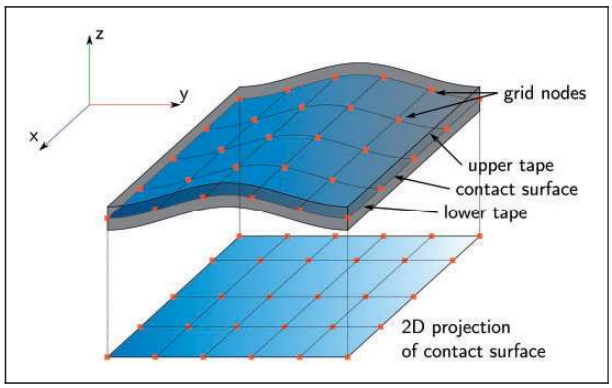

Figure 9. Grid nodes between an upper and a lower tape defining the contact layer and its projection to 2D.

Evaluation of contact from X-ray computed tomography measurements

The samples prepared in the consolidation experiments were investigated using X-ray computed tomography. Images were collected using a phoenix nanotom m 180 (beam current 200 µA, acceleration voltage 50 kV) with an integration time of 1500 ms. Between 9 and 14 samples were scanned simultaneously. For volume reconstruction, datos|x 2 reconstruction software package was used. The edge length of a voxel from the reconstructed volume was approximately 27 µm.

The contact surface between two tapes was determined from the reconstructed volume. Figure 9 schematically shows the contact surface between two tapes of one sample aligned parallel to the x–y plane. Taking in-plane bending into account, the contact surface was determined using a grid of nodes covering the whole contact surface. With increase in the bending of the sample, the number of grid nodes was increased to guarantee a well-approximated contact surface. From the grid nodes, the contact layer was determined by linear interpolation. Transformation from 3D to 2D representation was performed by parallel projection of the grayscale values within the contact surface as indicated in Figure 9.

The positions of the nodes between the tapes were determined from cross sections parallel to the y–z plane. One cross section showing nine samples stacked in z-direction is presented in Figure 10. The boundaries of the uppermost and the lowermost samples are highlighted in green and blue, respectively. In orange the grid nodes and their linear interpolation is shown between one tape–tape interface for each sample. The node positions were determined manually applying the following criteria: in case of gaps or absorption minima between the tapes, the node was located in the middle of the tapes. In case of no apparent gaps, the node was located between different oriented tapes.

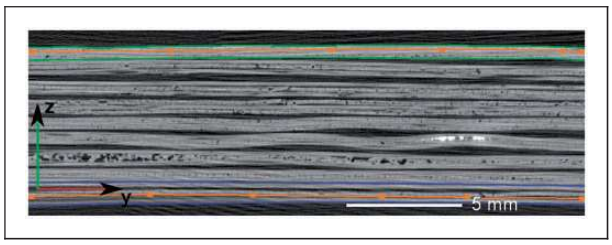

Figure 10. Virtual cross section parallel to the *y*–*z*-plane showing nine samples stacked in z-direction. The boundaries of the uppermost and the lowermost samples are highlighted in green and blue, respectively. The orange rectangular represent the nodes used for interpolation of the contact line between two tapes given in orange.

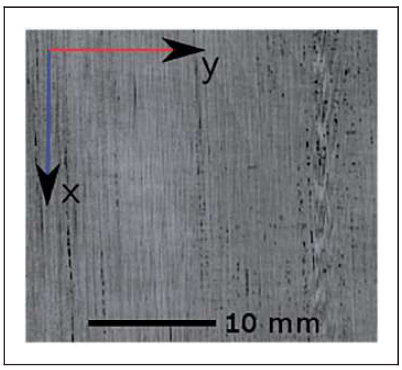

Figure 11. Contact surface between two tapes of the uppermost sample showing 96% of intimate contact.

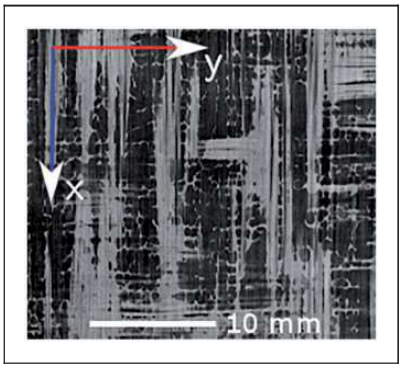

Figure 12. Contact surface between two tapes of the lowermost sample showing 44% of intimate contact.

The grayscale values of the contact surface were extracted using a plain projection parallel to the *x*–*y* plane. From the projection, the contact area was evaluated using Otsu's[22] threshold method. The grayscale values contributing to the brighter class were interpreted as contact. The degree of intimate contact was then calculated by the ratio of pixels corresponding to contact and total pixels of the evaluated surface. Examples for the contact planes for the uppermost sample and for the lowermost sample are shown in Figures 11 and 12, respectively.

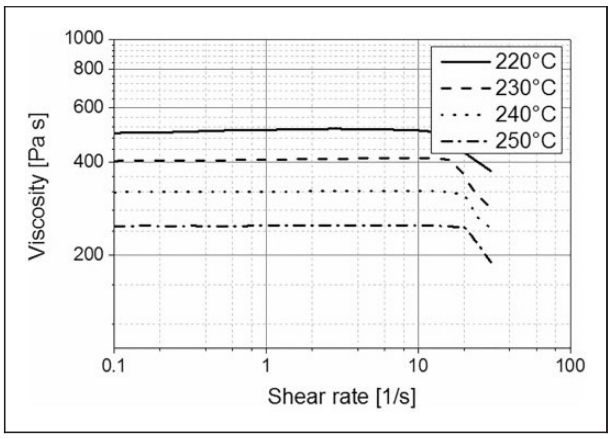

Figure 13. Viscosity measurements as function of temperature.

Results

In this section, we will first describe the evaluation of viscosity and the interlayer contact of the produced specimens from X-ray computed tomography images. Then, the model predictions of the Yang and Pitchumani model and Lee and Springer model will be presented and compared with the experimental results.

Viscosity of PA-6

Figure 13 shows the viscosity as function of the shear rate at different temperatures. The zero-shear-rate viscosity is 500 Pa s at 220°C and decreases with increasing temperature to 245 Pa s at 250°C. This is approximately 3–5 times smaller than typical values for PEEK at processing temperatures, which was explored in the previous studies.[7,12–14] The fiber–matrix viscosity of a reinforced PA-6 tape at 230°C is approximately 16,000 Pa s,[23] which is 40 times as high as the viscosity of the neat resin. During our experiments we also noticed that as soon as the material was molten some asperities were instantaneously annihilated, even without the application of pressure. The resin film near the surface melts and due to the surface energy of the liquid matrix a flat liquid film is formed.

The Arrhenius model parameters (equation (8)) obtained by these viscosity values are summarized in Table 3. These results are used for all further model predictions.

Evaluation of contact from X-ray computed tomography measurements

A cross section parallel to the *y*–*z* plane (Figure 9) of the reconstructed volume from X-ray computed

tomography from nine samples stacked in z-direction is shown in Figure 10. Increasing grayscale values correlate with increasing X-ray absorption. Therefore dark pixels contribute to voids or air, bright gray values to the composite, and white pixels can be assigned to the thermocouples. The stack shows a variety of different degrees of intimate contact. While the topmost of the nine specimens shows hardly any voids within the contact layer, the lowermost specimen still consists of three separated tape layers.

The projected contact layers are shown in Figures 11 and 12 for the topmost and lowermost sample, respectively. While in the sample showing high intimate contact the areas of no contact are limited to small spherical voids and laminar voids aligned in fiber direction, the sample with low intimate contact shows planar areas without contact. The evaluation of the degree of intimate contact provides a value of 96% and 44%, respectively.

Table 3. Parameters of the Arrhenius model.

Symbol	Unit	Value
A	Pa s	2.81×10^{-3}
E	J/mol	49,639.9
R	J/(mol K)	8.31

The development of the intimate contact by means of X-ray computed tomography is shown in Figures 14 and 15. The two figures visualize the same experimental data; however, the data are compared to the two different analytical models, which we chose for this study. Within each figure the experimental data for different pressures of 1000 Pa, 2000 Pa, and 4000 Pa at a temperature of 220°C as well as for different temperatures of 225°C and 230°C at a pressure of 1000 Pa are shown. The degree of intimate contact increased from 40% to full contact with increasing contact time. The timescale in which the intimate contact developments took place was in the range of a few seconds. For 1000 Pa and 220°C full contact was reached after 3–4 s, while the graphs at 2000 Pa and 4000 Pa show faster development of intimate contact at values of around 2–3 s. Due to inhomogeneous pressure distribution in the vicinity of the thermocouples the contact area was not developed completely in some cases.

We could observe that the development of intimate contact occurs faster with increasing temperature. The intimate contact was fully developed after 2–3 s at 225°C and 1000 Pa and in a time range below 1 s at 230°C. Times below 1 s could not be investigated due to handling limitations during the experiment. Therefore, samples manufactured at elevated temperatures showed an instantaneous development of intimate contact.

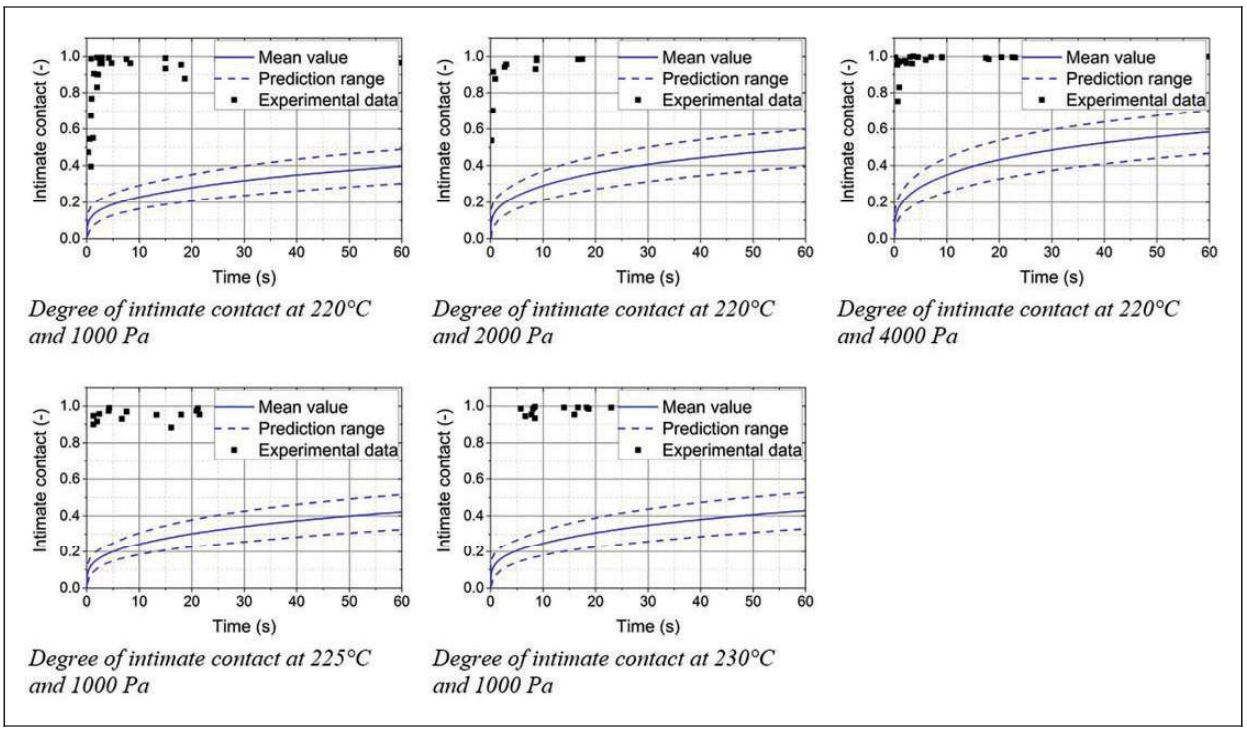

Figure 14. Experimental results and comparison with Yang and Pitchumani model.

Results of the Yang and Pitchumani contact model

The surface parameters were obtained as described in the "Material characterization" section and are summarized in Table 4. As explained earlier, the parameter D was determined from profilometry using the results of Dektak and AFM measurements. As shown in Figure 3, the surface profile shows fractal properties in a range from 4000 to 400,000 m^{-1}. The decrease in the slope of the power spectrum in the Dektak measurement is due to resolution limitations of the instrument. For error estimation the uncertainties from the fitting procedure was used. The difference in surface profiles obtained from AFM measurements at different positions of the tape's surface is negligible. The error of the Cantor set block length was estimated from the power spectrum. The error of the height of the first generation asperities was estimated from the standard deviation at three surface positions. Error in the scaling parameter was evaluated from the standard deviation of the scaling parameters obtained from different subareas of the surface profiles. The prediction range of the Yang and Pitchumani model was evaluated numerically: Random parameter sets were generated using Gaussian distributions of the parameter according to their mean values and errors. The development of intimate contact was calculated and subsequently, the average development and its standard deviation was given in the plots in Figure 14.

For 220°C and 1000 Pa, the model predicts an increase to an intimate contact of 40% in 60 s. The development of intimate contact is fast in the first seconds and the dynamic of the development decreases with time. The intimate contact reaches 100% after 33 min. The range of prediction covers a range of contact between 30% and 50% after 60 s. An increase in the consolidation pressure to 2000 Pa and 4000 Pa leads to an increase in contact of 40% and 50% after 60 s, respectively. Full contact is developed after 16 min at 2000 Pa and 9 min at 4000 Pa. There is no significant acceleration of the contact development when increasing the temperature to 225°C and 230°C. The model still predicts a contact of 42% and 43% compared to 40% at 220°C. Full contact is reached after 32 min and 28 min, respectively. For all these pressure temperature combinations, the prediction range is approximately ±10% due to uncertainties in the surface parameter determination.

Table 4. Surface parameters Yang and Pitchumani model.

Parameter	Unit	Mean value	Error
Fractal dimension, *D*		1.09	0.03
Height of first generation asperities, *h0*	μm	3.95	0.21
Scaling parameter, *f*		2.55	1.32
Cantor set block length	mm	0.25	0.06

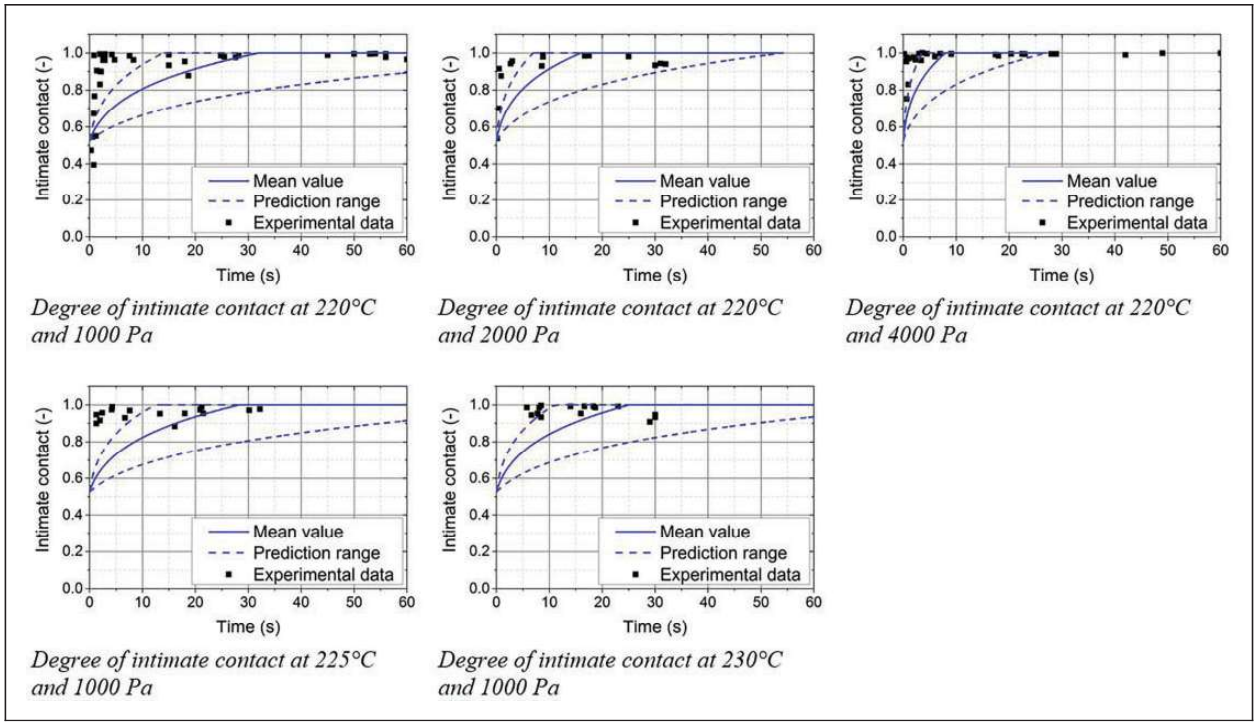

Figure 15. Experimental results and comparison with Lee and Springer model.

A comparison between the model's predictions and the experimental results show that the model is not capable of predicting the contact development between the two carbon fiber tapes using the surface parameters determined as described. While the experimental results indicate the development of full contact in the range of a few seconds the model predicts times in the range of a couple of minutes. And while the results indicate a significant acceleration of the contact development with increasing temperature the model is relatively insensitive to the temperature.

Results of the Lee and Springer contact model

The surface parameters for the model were obtained as described in the material characterization section and the results are summarized in Table 5.

The development of intimate contact according to equation (2) is highly sensitive to the surface parameters. The ratio of w_0 and b_0 characterizes the intercept of the D_{IC} curve with the y-axis, which is the initial intimate contact at the beginning of the consolidation. The ratio of a_0 and b_0 is the dominant surface parameter for the rate of contact development over time. Especially for low pressures and low temperatures the time needed to establish contact strongly depends on this rate of contact development. To account for the model's sensitivity, a minimum and maximum value for this ratio is calculated from the mean values of a_0 and b_0 and their standard deviation $\sigma(a_0)$ and $\sigma(b_0)$

$$\left(\frac{a_0}{b_0}\right)_{min} = \frac{a_{0,\,mean} - \sigma(a_0)}{b_{0,\,mean} + \sigma(b_0)} \tag{10}$$

$$\left(\frac{a_0}{b_0}\right)_{max} = \frac{a_{0,\,mean} + \sigma(a_0)}{b_{0,\,mean} - \sigma(b_0)} \tag{11}$$

The minimum and the maximum value describe the upper and lower boundary, respectively. The development of intimate contact predicted by the Lee and Springer model is shown in Figure 15. The figure shows the model predictions using the mean surface parameters and a lower and upper boundary for the development of intimate contact, which accounts for the uncertainties that occur in the parameter determination for the surface model.

Table 5. Surface parameters Lee and Springer model.

Parameter	Unit	Mean value	Error
a_0	µm	36.16	15.64
b_0	µm	179.95	87.18
w_0	µm	162.71	36.47

For all model predictions, the initial degree of intimate contact $D_{IC,0}$ is 52%. For the mean surface parameters, the following results from the model were obtained. At 220°C and a pressure of 1000 Pa, the development of intimate contact shows an asymptotical increase to 100% after 30 s. With increasing pressure, the contact development occurs faster at 15 s and 8 s for 2000 Pa and 4000 Pa, respectively. Increasing temperature increases the development of intimate contact to 28 s and 25 s at 225°C and 230°C, respectively. Decreases the time to reach full intimate contact to 28s and 25s at 225C and 230C, respectively.

Comparing the mean surface parameters with the upper and lower boundary, one can see that the time difference between the predicted mean consolidation time and the prediction of the upper and lower boundary decreases with an increase of pressure or temperature. For example, the time difference between the mean surface parameters and the upper boundary is 76 s for 1000 Pa and 220°C and decreases to 19 s for 4000 Pa and 220°C. This illustrates that for very low pressures and temperatures the model is very sensitive to the surface parameters, whereas the processing parameters become more dominant and therefore more relevant for higher pressures and temperatures.

Comparing the experimental data with the model predictions, the model (using the mean surface parameters) predicts a slower development of intimate contact than indicated by the experimental data, for most experimental points. Thus, the model does not precisely reflect the increase of contact over time. Nevertheless, the mean model prediction captures the the time scale, which is needed for full contact development.

Discussion

Timespan for development of intimate contact

In sum, our experimental results indicate that the contact development occurs fast during processing of carbon fiber reinforced PA-6, using low to moderate processing temperatures and very low pressures, compared to industrial processing parameters.

The fast development of intimate contact poses a challenge for consolidation experiments with low viscosity materials like PA-6. Longer consolidation times, like those of PEEK, are less prone to measurement errors.

Comparing our findings for the investigated tape material with results for PEEK tapes from the literature,[7,12–14,16] we conclude that the intimate contact development between carbon fiber reinforced PA-6 tapes takes place in only a fraction of time, which is due to the low viscosity of the matrix and probably the resin-rich layer at the tape surface.

For the evaluation of contact time a melting temperature threshold was used. Since the experimental results indicate that full contact development occurs in the range of 3–4 s even at melting temperature of 220°C, it is possible that the contact development continues even for temperatures below melting temperature. This phenomenon has recently been reported by Stokes-Griffin and Compston,[24] who investigated the bonding mechanisms during laser-assisted ATP of PEEK.

Accuracy of models in predicting contact development for PA-6 tapes

Overall, the Lee and Springer model as well as the Yang and Pitchumani model overestimated the time needed for the intimate contact to fully develop. One source for the discrepancy between the models' predictions and the experimental data could originate from the surface models and the surface parameter estimations. In our experiments with PA-6, we found differences in predictions of the two models: While the Lee and Springer model still allowed for a very conservative prediction of time needed to reach full intimate contact, the Yang and Pitchumani model significantly overestimated the time needed for contact development. Because the same model description for the mechanical deformation of the asperities as well as the identical viscosity was used, the difference between the two models presumably originates from the different assumptions regarding the surface representation.

One main difference in the surface parameter is that the identical rectangles model used by Lee and Springer shows a high initial degree of contact at 52% due to the nature of the surface representation, while the Cantor-Set representation of the surface in the model by Yang and Pitchumani leads to a large amount of small contact points with a low initial degree of contact. This difference could potentially cause the deviations in the predictions.

Regarding the two models we overall conclude that the Lee and Springer model delivered conservative results in all cases. Therefore, for the investigated PA-6 tapes it might be used to make worst case strength predictions especially in the static consolidation process such as thermoforming. However, in terms of the numerical process optimization of the automated tape placement both investigated analytical models do not seem not sufficiently accurate for the investigated material.

Limitations of the models with respect to surface parameter acquisition

Yang and Pitchumani model. One of the presumed advantages of the Yang and Pitchumani surface model is a distinct procedure for the acquisition of model parameters. Nevertheless, the advice given in the study of Yang and Pitchumani was deemed insufficient to provide a unique way of parameter determination. Especially, the fact that the determination of the parameters h_0 and f depends on the length of the considered surface profile or the type of background subtracted from the original data requires additional assumptions. The results indicate that high-resolution measurement methods, such as AFM, are not necessary to obtain the fractal dimensions of the surface, if the limitations of the used instruments are known in detail.

Lee and Springer model. For the Lee and Springer model no such distinct procedure exists to the authors' best knowledge. In our paper, we propose a method for determining the surface parameters for the model automatically from measured surface profiles. Compared to the previous studies in which surface parameters were fitted to experimental values,[16] this method allows a fast determination of the model parameters from tactile surface measurements. This method leads to a fairly good agreement between the experimental data and model predictions. Therefore, the proposed method is valid for tapes with a relatively smooth and uniform surface. However, it is important that the measured length of the profile is sufficiently large to capture the largest scale of asperities. For the investigated tapes the results were reproducible for measured lengths larger than 5000 μm. When smaller sections were analyzed, the obtained values for w_0 and b_0 were not representative.

Limitations of the models for low-viscous materials

One key parameter for the modeling of contact development is the viscosity of the material. It is important to identify whether the neat resin viscosity or the fiber resin viscosity of the tape is used to describe the deformation of the asperities during contact development. In this study, the neat resin viscosity was selected based on micrographs, which revealed a resin-rich layer near the surface of the investigated PA-6 tapes. In addition to the challenge of identifying the correct viscosity, both models assume deformation to occur due to pressure on the asperities. We found that the resin-rich molten surface also flattened without the application of pressure. The effect of surface flattening due to the surface energy of the molten polymer is not considered in the existing models but it could play an important role in explaining the difference between the experimental data and the model predictions.

Conclusions

An experimental study was conducted, which evaluated the intimate contact development between carbon

reinforced PA-6 tapes. The experimental results indicate that contact development takes place in the time range of a few seconds at temperatures only 10–20°C above the melting temperature of the matrix and pressures of 1–4 kPa. The experimental results were compared to two commonly used contact models. Our main conclusions are:

- While the Lee and Springer model provides a very conservative prediction of contact time, the Yang and Pitchumani model results in a significant overestimation of contact time for the investigated tape material.
- The results indicate that the assumptions, which are made for the viscosity of the material, are crucial for the quality of the prediction. The fiber distribution, namely the resin layer at the tape's surface fosters fast contact development.
- Since the viscosity of neat PA-6 is smaller than the viscosity of e.g. carbon fiber reinforced PEEK, additional effects such as surface energy should be considered for low-viscous materials.
- One major drawback for both analytical models is their sensitivity to the surface parameters. Not only are the models themselves very sensitive to a variation of surface parameters, the methods to obtain these parameters are also quite sensitive.

While the discussed models provide good results for different matrices, further experimental research with a larger variety of tape materials is needed to specify the fields of application of current intimate contact models.

Declaration of Conflicting Interests

The author(s) declared no potential conflicts of interest with respect to the research, authorship, and/or publication of this article.

Funding

The author(s) disclosed receipt of the following financial support for the research, authorship, and/or publication of this article: This study was funded by the German Federal Ministry of Education and Research (03MAI01L, 03MAI24C) within the leading edge cluster MAI Carbon.

Author contributions

The first and second authors have contributed equally to this work.

References

1. Henne F, Ehard S, Kollmannsberger A, et al. Thermoplastic in situ fiber placement for future rocket motor casings manufacturing. In: *SAMPE Europe technical conference 14*, Tampere, Finland, 10–11 September 2014, pp. 46–53.
2. Grouve WJB, Warnet LL, Rietman B, et al. Optimization of the tape placement process parameters for carbon–PPS composites. *Compos Part A: Appl Sci Manuf* 2013; 50: 44–53.
3. Bourban P-E, Bernet N, Zanetto J-E, et al. Material phenomena controlling rapid processing of thermoplastic composites. *Compos Part A: Appl Sci Manuf* 2001; 32: 1045–1057.
4. De Gennes PG. Reptation of a polymer chain in the presence of fixed obstacles. *J Chem Phys* 1971; 55: 572.
5. Bastien LJ and Gillespie JW. A non-isothermal healing model for strength and toughness of fusion bonded joints of amorphous thermoplastics. *Polym Eng Sci* 1991; 31: 1720–1730.
6. Ageorges C, Ye L and Hou M. Advances in fusion bonding techniques for joining thermoplastic matrix composites: A review. *Compos Part A: Appl Sci Manuf* 2001; 32: 839–857.
7. Khan MA, Mitschang P and Schledjewski R. Identification of some optimal parameters to achieve higher laminate quality through tape placement process. *Adv Polym Technol* 2010; 29: 98–111.
8. Ageorges C and Ye L. *Fusion bonding of polymer composites*, 1st ed. London: Springer, 2002, pp.105–114.
9. Tierney J and Gillespie JW Jr. Modeling of in situ strength development for the thermoplastic composite tow placement process. *J Compos Mater* 2006; 40: 1487–1506.
10. Pitchumani R, Gillespie JW and Lamontia MA. Design and optimization of a thermoplastic tow-placement process with in-situ consolidation. *J Compos Mater* 1997; 31: 244–275.
11. Sonmez FO and Akbulut M. Process optimization of tape placement for thermoplastic composites. *Compos Part A: Appl Sci Manuf* 2007; 38: 2013–2023.
12. Mantell SC and Springer GS. Manufacturing process models for thermoplastic composites. *J Compos Mater* 1992; 26: 2348–2377.
13. Lee WI and Springer GS. A model of the manufacturing process of thermoplastic matrix composites. *J Compos Mater* 1987; 21: 1017–1055.
14. Yang F and Pitchumani R. A fractal Cantor set based description of interlaminar contact evolution during thermoplastic composites processing. *J Mater Sci* 2001; 36: 4661–4671.
15. Dara PH and Loos AC. Thermoplastic matrix composite processing model. Technical Report 24061, Virginia Polytechnic Institute and State University, USA, 1985.
16. Levy A, Heider D, Tierney J, et al. Inter-layer thermal contact resistance evolution with the degree of intimate contact in the processing of thermoplastic composite laminates. *J Compos Mater* 2014; 48: 491–503.
17. Elson JM and Bennett JM. Calculation of the power spectral density from surface profile data. *Appl Opt* 1995; 34: 201–208.
18. Welch P. The use of fast Fourier transform for the estimation of power spectra: A method based on time averaging over short, modified periodograms. *IEEE Trans Audio Electroacoust* 1967; 15: 70–73.

19. Khanna YP and Kuhn WP. Measurement of crystalline index in nylons by DSC: Complexities and recommendations. *J Polym Sci Part B: Polym Phys* 1997; 35: 2219–2231.
20. Murthy NS, Kagan VA and Bray RG. Effect of melt temperature and skin-core morphology on the mechanical performance of nylon 6. *Polym Eng Sci* 2002; 42: 940–950.
21. Gröschel C and Drummer D. The influence of moisture and laminate setup on the de-consolidation behavior of PA6/GF thermoplastic matrix composites. *Int Polym Proc* 2014; 29: 660–668.
22. Otsu N. Threshold selection method from gray-level histograms. *IEEE Trans Syst Man Cybern* 1979; 1: 62–66.
23. Schaefer PM, Staden M, Zaremba S, et al. Material characterization for determining the consolidation properties of carbon fiber tapes with PA-6 matrix. In: *International conference on composite materials 20*, Copenhagen, Denmark, 19–24 July 2015, paper no. 5201-1.
24. Stokes-Griffin CM and Compston P. Investigation of sub-melt temperature bonding of carbon-fibre/PEEK in an automated laser tape placement process. *Compos Part A: Appl Sci Manuf* 2016; 84: 17–25.